Journal of Materials Chemistry B

PAPER

View Article Online
View Journal | View Issue

Cite this: J. Mater. Chem. B, 2017, 5, 6147

Facile size-controlled synthesis of fucoidan-coated gold nanoparticles and cooperative anticancer effect with doxorubicin†

Hongje Jang, [ab] Kyungtae Kang[c] and Mostafa A. El-Sayed*[a]

Received 25th April 2017,
Accepted 7th July 2017

DOI: 10.1039/c7tb01123g

rsc.li/materials-b

To conquer cancer, one of the most dangerous and common diseases faced by humanity, many therapeutic approaches have been researched and developed. Discovery of highly effective therapeutic molecules without side effects and novel strategies for their effective delivery are areas receiving recent global interest. Here, we describe a facile one-pot synthetic method for making gold nanoparticles coated with fucoidan, a natural product extracted from brown seaweed and a promising anticancer biopolymer. This nanoparticle formulation with well-controlled size distribution shows promise in enhancing the therapeutic and delivery efficacy. Moreover, stable surface modification of fucoidan coating followed by conjugation of doxorubicin through cleavable linkage significantly improved the anticancer effect. Fucoidan-coated gold nanoparticles containing doxorubicin exhibited more greatly enhanced anticancer effect than any other related platform following fucoidan-based cancer treatment adopting the nanoparticle integrated system.

1 Introduction

Fucoidan is a sulfated, fucose-rich polysaccharide, which is extracted from various brown algae and brown seaweed.[1] This sulfated polysaccharide is useful for many biological applications due to its properties including antiviral,[2–4] anticancer,[5] anti-proliferative,[6] anti-inflammatory,[7] immunomodulation,[8] anti-metastatic[9,10] and anticoagulant[11] effects and far more therapeutic advantages. Based on its diverse applicability and non-cytotoxicity, fucoidan has received a great deal of attention as a functional dietary supplement.

Cancer, the uncontrollable overgrowth and intemperate proliferation of genetically abnormal cells, is a dangerous and incurable disease.[12,13] Despite the remarkable research progress in cancer ecology and treatments, cancer is still one of the highest causes of mortality worldwide.[14] According to a report from the United States National Cancer Institute, approximately 1.6 million new cancer cases would be reported and 0.6 million people would be facing death from cancer in 2016 in the United States. To conquer cancer, countless therapeutic strategies have been reported and developed.[15–18] Of these, natural bioactive polysaccharides which have therapeutic effect have been shown to have good potential. In this regard, fucoidan has attracted clinical attention recently. This is based on its well-documented bioactive properties, including the p-glycoprotein-mediated drug efflux inhibition capability to resist multidrug resistance (MDR)[19] and activate autophagy,[20] and its autophagic cancer cell apoptosis ability, which suggest it to be a promising biopolymer for cancer therapy.[21–23] Moreover, cell cycle arrest at G1/S or G2/M phase by fucoidan is expected to give further help and aftercare in cancer treatment through its antiproliferative effect.[24,25] Conventionally, to conduct cancer chemotherapy using fucoidan, researchers use direct spreading of fucoidan onto various cancer targets such as breast cancer cells (MCF7 and MDA-MB-231),[26,27] cervical carcinoma (HeLa),[28] hepatocarcinoma (Huh7 and HepG2),[29] leukemia (HL60 and THP-1)[30] and lung cancer cells (A549),[31] and then confirm the excellent therapeutic effect from *in vitro* and *in vivo* tests. According to these reports, fucoidan successfully inhibits cancer cell growth, but further improvement is still required for selective and efficient cancer treatment applications.

Here, we synthesized fucoidan-coated gold nanoparticles (Fu-AuNPs) through a solvothermal one-pot approach. The size control of Fu-AuNPs was conveniently achieved by varying the concentration of fucoidan during the synthetic steps, and we successfully prepared fucoidan-coated gold nanospheres of between 15 and 80 nm in size. After the required characterizations of Fu-AuNPs to confirm the physicochemical properties of synthesized Fu-AuNPs, we accomplished chemical modification of the

[a] Laser Dynamics Laboratory, School of Chemistry and Biochemistry, Georgia Institute of Technology, Atlanta, GA 30332, USA. E-mail: melsayed@gatech.edu
[b] Department of Chemistry, Kwangwoon University, 20 Gwangun-ro, Nowon-gu, Seoul 01897, Republic of Korea
[c] Department of Applied Chemistry, Kyung Hee University, Yongin, Gyeonggi 17104, Republic of Korea

† Electronic supplementary information (ESI) available. See DOI: 10.1039/c7tb01123g

surface fucoidan coating of Fu-AuNPs to introduce bioconjugation-feasible aldehyde functional group-containing residues through the slight modification of a previous report. The prepared Fu-AuNPs were extremely stable at acidic/basic pH, at high salt concentration and in physiologically buffered solutions, to ensure further bio-applications. In the present study, in order to demonstrate the newly designed enhanced cancer therapeutic functions, we adopted cleavable Schiff base imine linkage-mediated doxorubicin bioconjugation onto acetylated Fu-AuNPs to maximize the synergistic effect between fucoidan (Fu: anti-cancer and multidrug resistance-inhibiting biopolymer) and doxorubicin (Dox: anticancer drug, topoisomerase II inhibitor) with a nanoparticle core. The advantages and novelty of this platform can be summarized as follows: (i) one-step facile synthesis of size-controlled Fu-AuNPs while maintaining colloidal stability, (ii) verification of enhanced cancer therapeutic efficiency of Dox-loaded Fu-AuNPs notwithstanding surface modification, (iii) selective anticancer effect of the Dox-Fu-AuNPs nanocomplex against cancer cells. There are several previous reports on fucoidan and gold nanoparticles for cancer treatment.[32,33] Compared with the previous reports, the current study provides advances as a cooperative model cancer therapy platform as follows: a series of studies on the synthesis of therapeutic polymer fucoidan-mediated gold nanoparticles with diameter control, surface modification and releasable drug conjugation for cancer therapy demonstrated by autophagosome immunostaining. In addition, the present approach can be a good use for another application of a therapeutic biopolymer to achieve the desired objective, a better treatment.

2 Experimental

2.1 Materials

Hydrogen tetrachloroaurate(III) hydrate, trisodium citrate dihydrate, sodium chloride, sodium hydroxide, pyridine, formamide, hydrogen chloride, acetic anhydride, doxorubicin hydrochloride, Hoechst 33342 and 2,3-bis-(2-methoxy-4-nitro-5-sulfophenyl)-2*H*-tetrazolium-5-carboxanilide (XTT) were purchased from Sigma-Aldrich (Milwaukee, WI, USA). Mozuku fucoidan extract powder was purchased from Okinawa Agent (Itoman, Japan). 10× phosphate-buffered saline (PBS), Dulbecco's modified Eagle's medium (DMEM) supplemented with 4.5 g L^{-1} glucose and sodium pyruvate, fetal bovine serum (FBS) and antimycotic solution were purchased from VWR (Radnor, PA, USA). Promo autophagy sensor LC3B-RFP BacMam 2.0 was purchased from Life Technology (Grand Island, NY, USA). All chemicals were used as received.

2.2 Synthesis of Fu-AuNPs

Fucoidan was dissolved in de-ionized (DI) water to prepare a 10 wt% stock solution. The solution was diluted to 0.5, 1.0, 1.5, 2.0 and 2.5 wt% in DI water with a total volume of 20 mL in glass vials, then heated up to 80 °C on a heat plate. To the sufficiently heated fucoidan solution, 20 μL of hydrogen tetrachloroaurate(III) hydrate stock solution (0.1 g mL^{-1}) was added and heated for an additional 2 h. The color of the reaction mixture turned from violet to red with increasing fucoidan content. The reaction mixtures were then cooled to room temperature under ambient conditions, then purified by centrifugation for 20 min at 8000 rpm. The product was rinsed four times with DI water to remove the remaining chemicals. Finally, synthesized Fu-AuNPs were re-dispersed in DI water and characterized by UV-vis spectrophotometry, then stored at room temperature. The Fu-AuNPs should be consumed within one month to prevent aggregation due to colloidal stability decrement.

2.3 Synthesis of citrate-stabilized AuNPs

Fifty milliliters of 0.25 mM hydrogen tetrachloroaurate(III) solution was heated to boiling and an appropriate volume of 34 nM trisodium citrate dehydrate solution was then added. The reaction mixtures were boiled for an additional 20 min until the color changed to red-violet depending on particle size, similar to Fu-AuNPs, and then cooled to room temperature. Synthesized AuNPs were re-dispersed in DI water and characterized by UV-vis spectrophotometry, then stored at room temperature.

2.4 Characterization of synthesized nanoparticles

A JEOL TEM 100CX (JEOL, USA) was used to obtain images of AuNPs. Particle size distribution and zeta potential were determined by Zetasizer NS90 (Malvern, UK). Fluorescence images of cells were collected by a Zeiss LSM 700-405 confocal microscope (Carl Zeiss Inc., Oberkochen, Germany). Absorbance measurement during XTT assay was performed using a Synergy Mx (BioTek, UK).

2.5 Surface modification of Fu and Fu-AuNPs

To conduct surface modification to introduce aldehyde functional groups (Ac) for further bioconjugation processes, Fu-AuNPs dispersed in DI water were mixed with formamide with a ratio of 3 : 1 DI water : formamide. To the mixture, 50 μL of pyridine and 150 μL of acetic anhydride were added sequentially. After vigorously vortexing for 1 min, the mixed solution was incubated for 12 h at room temperature with periodic vortexing every 2 h. The product was collected by centrifugation at 5000 rpm for 10 min, then washed with DI water more than 4 times. The product was characterized by UV-vis spectrophotometry to check stability maintenance without aggregation formation. In the case of free fucoidan, the reaction product was purified using a centrifuge filter tube to remove remaining chemicals conveniently. The final products were stored at room temperature for the subsequent drug conjugation process.

2.6 Doxorubicin conjugation onto Ac-Fu and Ac-Fu-AuNPs

To accomplish drug loading onto the chemically modified surface of Ac-Fu and Ac-Fu-AuNPs, doxorubicin hydrochloride was directly added to Ac-Fu and Ac-Fu-AuNPs. To the mixture, a small portion of sodium hydroxide solution was added to adjust the pH to near 10 (basic) for Schiff base imine linkage formation. The mixture was incubated for at least 12 h at room temperature, then purified by centrifugation to remove unbound Dox from the solution. The drug-conjugated compound should be consumed directly after preparation, and when storage is needed

the product should be stored in a slightly basic environment to maintain the imine linkage-mediated conjugation.

2.7 Doxorubicin loading and release profiling

After collection of the drug conjugation compound by centrifugation, the precipitate was rinsed with pH 10 buffered solution to prevent imine bond breakage and all the supernatant was collected. The amount of dissolved Dox in the supernatant was measured by absorption at 488 nm ($\varepsilon_{Dox,488}$ = 11 500 L mol^{-1} cm^{-1}) and calculated by means of the Beer–Lambert law. To monitor the release of the loaded Dox in neutral and acidic pH conditions, the Dox-Ac-Fu-AuNPs were dispersed in citrate buffer (pH 5.0) and phosphate-buffered saline (pH 7.4) at room temperature. At designated time points, the solutions were centrifuged at 10 000 rpm for 5 min to precipitate the nanoparticles, and the Dox concentration in the supernatant due to drug release was determined by absorbance measurement at 488 nm using the same procedure as above. These measurements were repeatedly performed to get the release profile data set.

2.8 Cell culture

Human oral squamous cell carcinoma (HSC3) cells and human keratinocyte (HaCaT) cells were cultured in Dulbecco's modified Eagle's medium supplemented with 4.5 g L^{-1} glucose and sodium pyruvate, 10% v/v fetal bovine serum and 1% antimycotic solution. Cell cultures were maintained at 37 °C in a 5% CO_2 humidified incubator.

2.9 XTT assay for cell viability measurement

HSC3 and HaCaT cells were seeded with a density of 5000 cells per well in a 96-well culture plate with 100 μL of growth medium (about 50% confluence). After the successful cell attachment after 1 day of incubation, nanoparticles or drug–nanoparticles were added to conduct cell viability assays. The cells were incubated for an additional 24 or 48 h under the incubation conditions (37 °C, 5% CO_2 humidity), and then rinsed with 1× PBS. Fifty microliters of activated XTT solution (XTT solution + activation reagent) was added to each well and the plate was incubated in an incubator for an additional 4 h. The plate was shaken gently to evenly distribute the dye in the wells, then the absorbance of the samples was measured with a spectrophotometer at a wavelength of 450–500 nm with reference absorbance at 630–690 nm. Mean and standard deviation of triplicates were calculated and plotted.

2.10 Confocal laser scanning microscopy measurement

HSC3 and HaCaT cells were seeded at a density of 10 000 cells per coverslip onto round glass coverslips located in a 12-well culture plate with 1 mL of growth medium. After 1 day of incubation to ensure cell attachment, the cells were treated with nanoparticles or drug–nanoparticles and then incubated for an additional 24 h at 37 °C, 5% CO_2 humidity. The culture medium was discarded, then Hoechst 33342 nuclei staining was performed. After 2 h, the cells were rinsed with 1× PBS and observed by confocal laser scanning microscopy using a Zeiss LSM 700-405 confocal microscope.

3 Results and discussion

3.1 Synthesis and characterization of Fu-AuNPs

First, the fucoidan-coated AuNPs (Fu-AuNPs) were synthesized by a solvothermal method similar to a previously reported AuNPs synthetic approach using polysaccharide (Fig. 1a).[34,35] Briefly, the mixing of $AuCl_4^-$ and fucoidan extract solution was followed by heating for 2 h at 80 °C, which induced the reduction of Au(III) ions into gold nanoparticles (AuNPs) through the binding to and subsequent reduction by hydroxyl functional groups of fucoidan chains. The completion of Fu-AuNPs formation was clearly identified by the change of distinctive surface plasmon resonance (SPR) band and solution color (Fig. 1b and c). In order to establish the dependence of diameter, morphology and distribution of formed nanoparticles on reaction conditions, we conducted the Fu-AuNPs synthesis using 0.5, 1.0, 1.5, 2.0 and 2.5 wt% fucoidan concentrations.

Because, in the present platform, fucoidan plays key roles as a reducing agent for gold ions and a surface coating material, we set only the concentration of fucoidan as a variable parameter. As a result, UV-vis spectrophotometry of synthesized Fu-AuNPs clearly showed an SPR red shift from 527.5 to 556.5 nm, which was closely related to diameter increase, with reduction of fucoidan concentration from 2.5 wt% to 0.5 wt%. Additionally, we performed transmission electron microscopy (TEM) and dynamic light scattering (DLS) characterization to verify the diameter and morphological characteristics of the formed Fu-AuNPs with surface fucoidan coating. According to the TEM observations, as the concentration of fucoidan extract was increased (0.5, 1.0, 1.5, 2.0 and 2.5 wt%), average diameters of nanoparticles declined (83 ± 11.6, 52 ± 8.2, 35 ± 1.9, 22 ± 2.4, and 15 ± 1.5 nm, respectively) with a wide diameter distribution range and accretion of anisotropic nanostructures such as

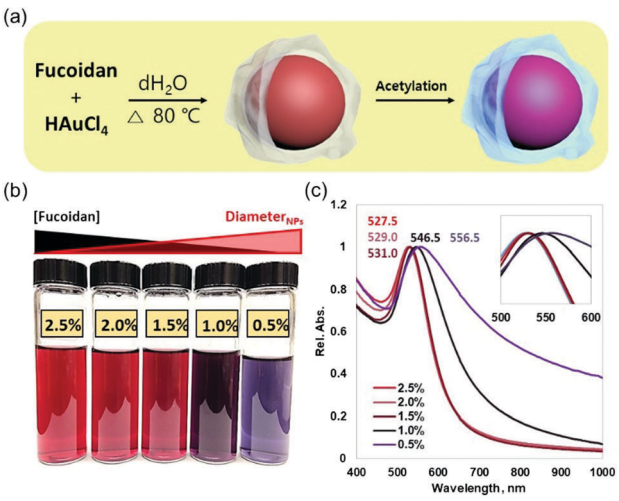

Fig. 1 Synthesis of Fu-AuNPs by solvothermal method. (a) Schematic illustration of Fu-AuNPs synthesis and surface modification. (b) Photographs of prepared Fu-AuNPs with different diameters. Each Fu-AuNPs sample exhibited a distinctive color derived from the particle diameter. (c) UV-vis spectra of prepared Fu-AuNPs. Along with the diameter increase, SPR red shifts were clearly observed from 527.5 up to 556.5 nm.

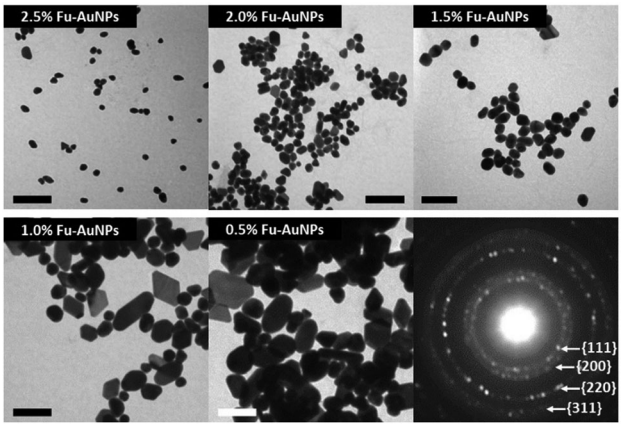

Fig. 2 Transmission electron microscope images of prepared Fu-AuNPs with different diameter distribution. As the concentration of fucoidan increased, the diameter of synthesized Fu-AuNPs showed a decreasing tendency with higher monodispersity. Selected-area electron diffraction (SAED) as shown in the bottom right panel also supported the formation of well-crystallized AuNPs from fucoidan-mediated synthesis. All scale bars are 100 nm.

nanoplates (Fig. 2). DLS analysis presented significantly higher hydrodynamic radii of 120 ± 28.5, 75 ± 16.6, 50 ± 10.3, 45 ± 7.2, and 38 ± 5.4 nm in comparison with the diameters derived from TEM images (Fig. S1a, ESI†). The big difference in measured diameter between TEM and DLS strongly supports the presence of a surface-adsorbed fucoidan layer. Additionally, the lower zeta potential of smaller Fu-AuNPs implied a relatively higher amount of fucoidan deposition than for larger Fu-AuNPs, inferred to be due to the negative charge of fucoidan due to sulfated residues (Fig. S1, ESI†). Higher than 2.5 wt% of fucoidan did not result in diameter change, and lower than 0.5 wt% of fucoidan only formed unstable Fu-AuNPs that aggregated during reaction.

3.2 Colloidal stability confirmation

Next, we performed colloidal stability assessment to verify the bio-application feasibility of Fu-AuNPs. Here, various sized Fu-AuNPs were mixed with diverse test solutions to measure colloidal stability against acidic/basic pH, high salt concentrations and physiological buffer solution 1× phosphate-buffered saline (1× PBS, composition 137 mM NaCl, 2.7 mM KCl, 4.3 mM Na_2HPO_4 and 1.47 mM KH_2PO_4, pH 7.4). The stability decrements over time were observed by UV-vis spectrophotometry and digital photograph images. The smaller Fu-AuNPs exhibited well-preserved colloidal stability and robustness against all test conditions up to 24 h of incubation at room temperature, unlike the larger Fu-AuNPs (1.0 and 0.5 wt% Fu-AuNPs) which formed aggregates in 1000 mM NaCl solution. Taking together the colloidal stability of Fu-AuNPs and aggregation at 0.5 wt% fucoidan concentration during synthesis, we concluded fucoidan serves not only as reducing agent but also indeed as surface stabilizer. As a result, 2.5, 2.0 and 1.5 wt% Fu-AuNPs could be the optimized nanomaterials for various bio-applications, which require pH and salt durability (Fig. S2 and S3, ESI†).

3.3 Acetylation of Fu-AuNPs

Surface fucoidan residues of prepared Fu-AuNPs were chemically acetylated to introduce aldehyde functional groups by a previously reported approach with slight modification in reaction conditions.[36,37] Briefly, Fu-AuNPs dispersed in deionized (DI) water after sufficient purification were mixed with formamide, then pyridine and acetic anhydride were added followed by vigorous mixing for 1 min. The mixed solution was incubated for 12 h at room temperature with periodic vortexing every 2 h. The product was collected by centrifugation at 5000 rpm for 10 min then washed with DI water more than 4 times. The product was characterized by UV-vis spectrophotometry to check the stability following surface modification reaction. Fu-AuNPs did not exhibit any aggregation or distinctive SPR shift through the modification. The acetylation of Fu-AuNPs was also confirmed by Fourier transform infrared (FT-IR) spectroscopy. By comparing the FT-IR spectra of Fu-AuNPs and Ac-Fu-AuNPs, we observed an increase of the carboxyl –C═O peak at 1639 cm^{-1} and decrease of the hydroxyl –OH band around 3327 cm^{-1} resulting from acetylation (Fig. S4, ESI†).

3.4 Doxorubicin loading onto and release from Ac-Fu-AuNPs

To assess the acetylation of surface fucoidan of Fu-AuNPs, we next performed Dox loading onto acetylated Fu-AuNPs and calculated the loading capacity. The loading of Dox was achieved by Schiff base linkage formation between amine functional group of Dox and aldehyde functional group of the acetylated fucoidan coating on the Fu-AuNPs (Ac-Fu-AuNPs), and it could be considered indirect evidence of surface fucoidan modification. After the mixing of 10 μM Dox with each size of Fu-AuNPs and Ac-Fu-AuNPs containing 1 mg μL^{-1} fucoidan (proportionally 1000 equivalents on a molar basis), a sufficient incubation time was allowed for imine linkage-based Dox loading. The product was purified by centrifugation and the supernatant was collected for detection of unbound Dox by UV-vis spectrophotometry. During 24 h of incubation at room temperature, we periodically separated out the existing Dox-Ac-Fu-AuNPs by centrifugation and measured the absorption spectrum of unbound Dox at 480 nm in the supernatant to track the loading profile against time. The calculation of the amount of Dox was accomplished using the Beer–Lambert law and the reported extinction coefficient of Dox. According to the comparison with the initial amount of Dox, all Dox was successfully loaded onto Ac-Fu-AuNPs within 24 h and loading was completed faster with the smaller Fu-AuNPs which contain a higher fraction of fucoidan (Fig. 3a). The amounts of Dox loaded onto Fu-AuNPs and Ac-Fu-AuNPs after 24 h of incubation were calculated as 6.5% and 99%, respectively, from UV-vis absorption spectra (Fig. 3b). The Dox loading capacity considered together with reliability data demonstrated the successful acetylation of surface fucoidan of Fu-AuNPs with effective numbers of aldehyde functional groups for imine-based drug-loading activation.

The acid-triggered imine bond breakage and following release of loaded cargo form a well-established strategy to conduct drug delivery. Therefore, we designed a release efficiency test in

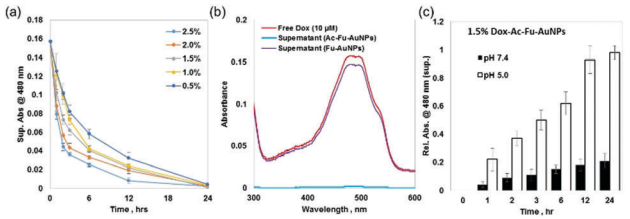

Fig. 3 Characterization of loading of Dox onto acetylated Fu-AuNPs and acidic environment-triggered release profile of conjugated Dox. (a) Loading profile of Dox on various sized Ac-Fu-AuNPs by Schiff base imine linkage. The Dox loading was calculated by measurement of absorbance at 480 nm of the supernatant after centrifugation to sediment the formed Dox-Ac-Fu-AuNPs complex. (b) UV-vis absorption spectra of Ac-Fu-AuNPs and Fu-AuNPs supernatant after centrifugation with the same concentration of free Dox. Significant loading capacity is presented. (c) Release profile of 1.5 wt% Dox-Ac-Fu-AuNPs in acidic (pH 5.0) and neutral (pH 7.4) solutions. The acidic environment exhibited 5 times higher releasing efficiency than the neutral condition at 24 h of incubation.

cytosol (pH 7.4) and endosomal/lysosomal (pH 5) mimetic pH-buffered solutions by using UV-vis spectrophotometry of the supernatant after sedimenting the remaining Dox-Ac-Fu-AuNPs complex by centrifugation. According to the release profile of Dox, almost all the Dox loaded by imine bonding was totally released within 24 h at the acidic pH, unlike in the case of neutral pH, which exhibited just 20% of maximum release at the same measurement time (Fig. 3c and Fig. S5, ESI†).

3.5 Cytotoxicity assay of Fu-AuNPs

Prior to the therapeutic efficacy assay, we performed cytotoxicity measurement of Fu-Ac-AuNPs to demonstrate the anticancer effect of fucoidan against human oral squamous carcinoma cells (HSC3) and human keratinocyte cells (HaCaT) by 2,3-bis-(2-methoxy-4-nitro-5-sulfophenyl)-2*H*-tetrazolium-5-carboxanilide (XTT) assay. XTT assays of cells treated with therapeutically efficient molecules including only free fucoidan (free Fu), free Dox and Dox-Ac-Fu complex without nanoparticles presented significant difference in the case of fucoidan-involved experimental sets. Dox-Ac-Fu complex was prepared by the same protocol with surface modification and Dox conjugation as Dox-Ac-Fu-AuNPs. Relative cell viabilities of free Fu and Dox-Ac-Fu treatments were calculated as 1.225 (HaCaT)/0.725 (HSC3) and 0.831 (HaCaT)/0.408 (HSC3), respectively, in contrast with free Dox treatment which exhibited similar cell viabilities of 0.962 (HaCaT)/0.823 (HSC3). Thus, fucoidan served not only as an anticancer drug but also as a synergistic therapeutic biopolymer with Dox (Fig. 4a). To confirm the selective anticancer effect of Ac-Fu-AuNPs, various sized Ac-Fu-AuNPs were added to HaCaT and HSC3 cells followed by XTT assay. As a result, all the Fu-AuNPs (0.5, 1.0, 1.5, 2.0 and 2.5 wt%) induced noticeable difference in cell viability against HaCaT and HSC3 cells. Ac-Fu-AuNPs treatment showed a cell viability of less than 50% in HSC3 cells, whereas HaCaT cells exhibited cell proliferation rather than apoptosis. The selective anticancer effects of fucoidan that we observed were consistent with previous reports on fucoidan derivative research.[38,39] Moreover, the greater anticancer efficiency

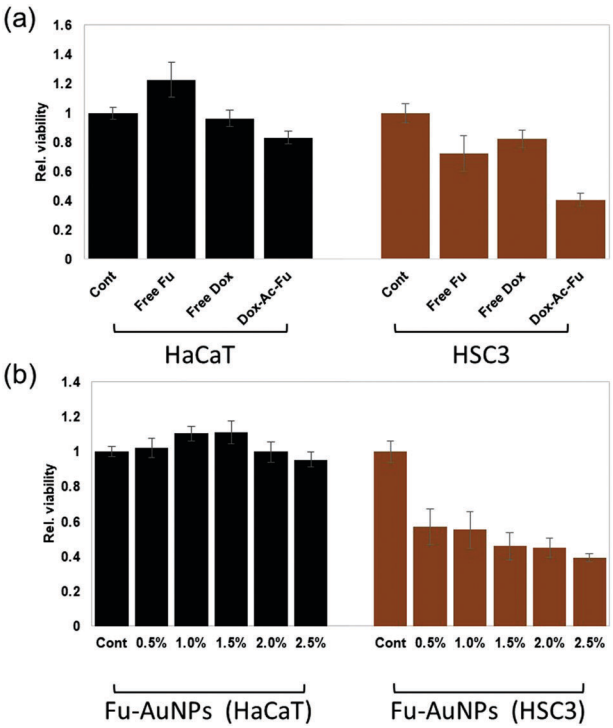

Fig. 4 Verification of anticancer effect of Fu-AuNPs. (a) To confirm the anticancer effect of fucoidan and its synergistic effect with Dox loading, free Fu, free Dox and Dox-Fu drug–polymer complex without nanoparticle core were added to normal cells (HaCaT) and cancer cells (HSC3). It was clearly shown that Fu has a much more selective anticancer effect than Dox. The amounts of drugs used for treatment were 100 mg mL^{-1} Fu and/or 100 μM Dox, respectively. (b) Anticancer effect of Fu-AuNPs was measured against HaCaT and HSC3 cells. All of the Fu-AuNPs showed an anticancer effect, and smaller particles which had more Fu exhibited higher anticancer effect in equal concentration treatments. The relative cell viability was calculated by comparison with untreated control set (denoted Cont).

of smaller Fu-AuNPs derived from higher fucoidan concentration supported the major role of fucoidan as an anticancer agent (Fig. 4b).

3.6 Cooperative cancer treatment efficacy of Dox-Ac-Fu-AuNPs

Further, we investigated the individual anticancer effects of free Fu, free Dox and Dox-Ac-Fu as a control experiment for clarifying the cooperative anticancer effect of Ac-Fu-AuNPs and Dox-Ac-Fu-AuNPs through the calculation of EC_{50} (concentration of drug that gives half-maximal response). According to the XTT assay against HSC3 cells, EC_{50} was calculated as 134.4 μg μL^{-1}, 2744.5 nM and 76.5 μg Fu μL^{-1}, respectively, for free Fu, free Dox and Dox-Ac-Fu complex by using four-parameter logistic nonlinear regression to data points. From these calculations, Dox-Ac-Fu exhibited 175.7% lower EC_{50} value than free Fu, and presented 57% decreased cell viability relative to free Dox at the same concentration (Fig. S6, ESI†). These EC_{50} values implied the existence of a cooperative anticancer effect between fucoidan and Dox. For direct comparison of therapeutic efficacy of Ac-Fu-AuNPs and Dox-Ac-Fu-AuNPs, we treated HSC3 cells with Dox-Ac-Fu-AuNPs (prepared using 1000 eq. $n_{Dox}/n_{Fu\text{-}AuNPs}$) and the same

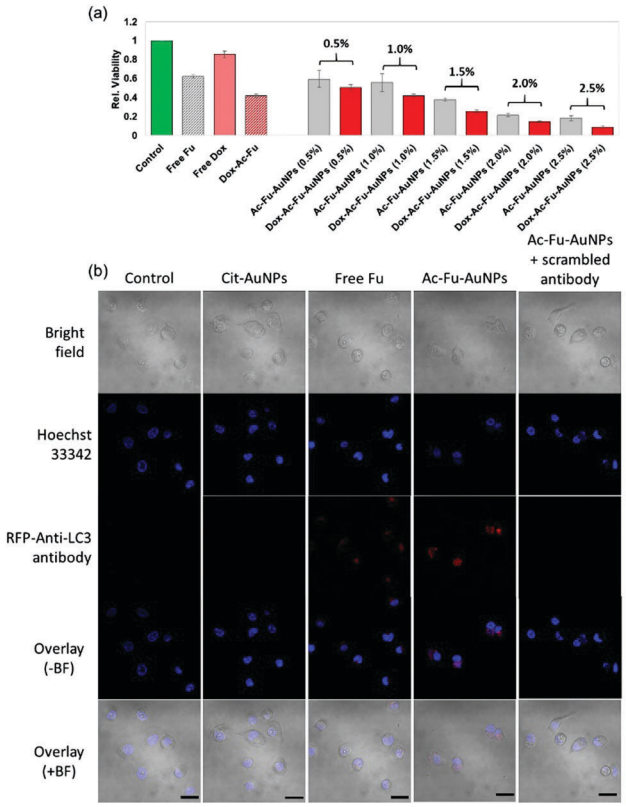

Fig. 5 Quantitative viability comparison of various Dox-Ac-Fu-AuNPs and Ac-Fu-AuNPs against HSC3 cells to verify the synergistic anticancer effect. (a) Ac-Fu-AuNPs showed higher anticancer effect than free Fu (without nanoparticle core), and Dox loading gave additional enhancement of the anticancer effect. Especially, smaller Ac-Fu-AuNPs showed stronger anticancer effect than larger ones. The amounts of loaded cargos were 100 mg mL^{-1} Fu and 100 μM Dox, respectively. The relative cell viability was calculated by comparison with the untreated control set (denoted Control). (b) Fluorescence microscope images to check autophagy due to the fucoidan moiety. The notation 'scrambled antibody' implies treatment with inefficiently LC3-recognizable control antibody reagent. BF is the abbreviation for bright field image. The scale bars represent 20 μm.

concentration of Ac-Fu-AuNPs, then incubated for 24 h followed by XTT assay with sevenfold replication. According to the relative cell viability data especially focused on each sized set of Dox-Ac-Fu-AuNPs, all of the Dox-Ac-Fu-AuNPs produced lower cell viability than Ac-Fu-AuNPs: 50.4%/59.4% (0.5 wt%), 42.2%/55.8% (1.0 wt%), 25.5%/38.2% (1.5 wt%), 14.4%/21.7% (2.0 wt%) and 9.0%/18.3% (2.5 wt%). Normalized to the molarity of Ac-Fu-AuNPs, the EC_{50} values of Dox-Ac-Fu-AuNPs and Ac-Fu-AuNPs were 99.2/230.5 (0.5 wt%), 115.4/161.3 (1.0 wt%), 45.6/69.3 (1.5 wt%), 25.8/40.5 (2.0 wt%) and 22.6/37.7 pM (2.5 wt%) (Fig. S7, ESI†). The lower viability measured from Dox-Ac-Fu-AuNPs than Ac-Fu-AuNPs and increasing anticancer effect proportional to the fucoidan content clearly meant existence of a cooperative anticancer effect. Moreover, comparing Dox-Ac-Fu and Dox-Ac-Fu-AuNPs, which represented the presence and absence of the gold nanoparticle core, Ac-Fu-AuNPs and Dox-Ac-Fu-AuNPs presented better therapeutic effect than free Fu (62.0%) and Dox-Ac-Fu (41.9%) treatment (Fig. 5a). This difference in anticancer effect originates from the ease of internalization, accumulation in the endosome and faster encounter with late endosome or lysosome to initiate acid-triggered drug release for nuclear delivery from inside the cell. To visualize fucoidan working against the cancer cells through autophagic cell death, we stained the cells with Hoechst 33342 (nuclear, blue signal in Fig. 5b) and RFP-anti-LC3-antibody (autophagosome, red signal in Fig. 5b) followed by observation with fluorescence microscope. It was clear that the presence of both fucoidan and active RFP-anti-LC3-antibody was necessary to induce strong red fluorescence emission from the autophagosome–autolysosome, located in the perinuclear region (Fig. 5b).

4 Conclusions

In conclusion, we synthesized various sized Fu-AuNPs using the anticancer biopolymer fucoidan through a solvothermal reduction method and successfully performed surface modification of the nanoparticles to introduce aldehyde groups for further bioconjugation. The Fu-AuNPs were extremely stable against acidic/basic pH, high salt concentration and physiological buffered solutions. To utilize the synergistic effect of autophagic cancer cell apoptosis and multidrug resistance of fucoidan, we loaded Dox onto the surface acetylated fucoidan coating of Fu-AuNPs by imine linkage, which can be broken by acid-catalyzed reaction. As we expected, Dox-Ac-Fu-AuNPs exhibited excellent therapeutic effect against a cancer cell line (HSC3) selectively. We forecast that the present one-pot synthetic method of making biopolymer-coated gold nanoparticles with size control will become one of the most convenient and robust methods to design functional nanomaterials, combined with surface modification and bioconjugation. It is one of the most promising options for synergistic cancer therapy application in the near future.

Acknowledgements

This work was supported by National Institutes of Health (NIH)-National Cancer Institute (NCI) grant U01CA151802. This study was supported by grant no. NRF-2016R1C1B1008090.

Notes and references

1 P. Bhadury, B. T. Mohammad and P. C. Wright, *J. Ind. Microbiol. Biotechnol.*, 2006, **33**, 325–337.
2 T. Toshihiko, C. Amornrut and J. L. Robert, *Trends Glycosci. Glycotechnol.*, 2003, **15**(81), 29–46.
3 M. Baba, R. Snoec, R. Pauwels and D. E. Clercq, *Antimicrob. Agents Chemother.*, 1988, 1742–1745.
4 M. Hasui, M. Matsuda and K. Okutani, *Int. J. Biol. Macromol.*, 1995, **17**, 293–297.
5 X. Z. Wu and D. Chen, *West Indian Med. J.*, 2006, **4**, 270–273.
6 L. S. Costa, G. P. Fidelis, S. L. Cordeiro, R. M. Oliveira, D. A. Sabry, R. B. Camara, L. T. Nobre, M. S. Costa, J. Almeida-Lima, E. H. Farias, E. L. Leite and H. A. Rocha, *Biomed. Pharmacother.*, 2010, **64**, 21–28.

7 M. S. Matsui, N. Muizzuddin, S. Arad and K. Marenus, *Appl. Biochem. Biotechnol.*, 2003, **104**, 13–22.
8 I. Wijesekara, R. Pangestuti and S. K. Kim, *Carbohydr. Polym.*, 2011, **84**, 14–21.
9 R. C. Pariah, C. Freeman, J. K. Brown, D. J. Francis and W. B. Cowden, *Cancer Res.*, 1999, **59**, 3433–3441.
10 X. Tang, J. Li, X. Xin and M. A. Geng, *Cancer Biol. Ther.*, 2006, **5**(11), 1474–1480.
11 V. H. Pomin, *Biopolymers*, 2009, **91**(8), 601–609.
12 D. Hanahan and R. A. Weinberg, *Cell*, 2011, **144**(5), 646–674.
13 National Cancer Institute, *Defining Cancer*, retrived 10 June 2014.
14 World Health Organization, *World Cancer Report*, 2014, ch. 1, p. 1.
15 C. K. Bomford and I. H. Kunkler, *J. Walter and Miller's Textbook of Radiotherapy: radiation physics, therapy, and oncology*, 6th edn, 2003, p. 311.
16 T. A. Waldmann, *Nat. Med.*, 2003, **9**(3), 269–277.
17 B. R. Cassileth and G. Deng, *Oncologist*, 2004, **9**(1), 80–89.
18 A. Vickers, *Ca-Cancer J. Clin.*, 2004, **54**(2), 110–118.
19 A. Bernkop-Schnurch and V. Grabovac, *Am. J. Drug Delivery*, 2006, **4**(4), 263–272.
20 S. Chen, Y. Zhao, Y. Zhang and D. Zhang, *PLoS One*, 2014, **9**(9), e108157.
21 M. T. Ale, H. Maruyama, H. Tamauchi and J. D. Mikkelsen, *Int. J. Biol. Macromol.*, 2011, **49**, 331–336.
22 T. Teruya, T. Konishi, S. Uechi, H. Tamaki and M. Tako, *Int. J. Biol. Macromol.*, 2007, **41**, 221–226.
23 Y. Liang, C. Yan and N. F. Schor, *Oncogene*, 2001, **20**, 6570–6578.
24 S. Fukahori, H. Yano, J. Akiba, S. Ogasawara, S. Momosaki, S. Sanada, K. Kuratomi, Y. Ishizaki, F. Moriya and M. Yagi, *Mol. Med. Rep.*, 2008, **1**(4), 537–542.
25 K. Haneji, T. Matsuda, M. Tomita, H. Kawakami, K. Ohshiro, J. N. Uchihara, M. Masuda, N. Takasu, Y. Tanaka, T. Ohta and N. Mori, *Nutr. Cancer*, 2005, **52**(2), 189–201.
26 Z. Zhang, K. Teruya, H. Eto and S. Shirahata, *PLoS One*, 2011, **6**(11), e27441.
27 A. Cumashi, N. A. Ushakova, M. E. Preobrazhenskaya, A. D'Incecco, A. Piccoli, L. Totani, N. Tinari, G. E. Morozevich, A. E. Berman, M. I. Bilan, A. I. Usov, N. E. Ustyuzhanina, A. A. Grachev, C. J. Sanderson, M. Kelly, G. A. Rabinovich, S. Iacobelli and N. E. Nifantiev, *Glycobiology*, 2007, **17**(5), 541–552.
28 Z. Zhang, K. Teruya, H. Eto and S. Shirahata, *Biosci., Biotechnol., Biochem.*, 2013, **77**(2), 235–242.
29 T. Nagamine, K. Hayakawa, T. Kusakabe, H. Takada, K. Nakazato, E. Hisanaga and M. Iha, *Nutr. Cancer*, 2009, **61**, 340–347.
30 J. O. Jin, M. G. Song, Y. N. Kim, J. I. Park and J. Y. Kwak, *Mol. Carcinog.*, 2010, **49**, 771–782.
31 H. Lee, J. S. Kim and E. Kim, *PLoS One*, 2012, **7**(11), e50624.
32 M. Tengdelius, D. Gurav, P. Konradsson, P. Pàhlsson, M. Griffith and O. P. Oommen, *Chem. Commun.*, 2015, **51**, 8532–8535.
33 P. Manivasagan, S. Bharathiraja, N. Q. Bui, B. Jang, Y. O. Oh, I. G. Lim and J. Oh, *Int. J. Biol. Macromol.*, 2016, **91**, 578–588.
34 H. Jang, Y. K. Kim, S. R. Ryoo, M. H. Kim and D. H. Min, *Chem. Commun.*, 2010, **46**, 583–585.
35 H. Jang, S. R. Ryoo, K. Kostarelos, S. W. Han and D. H. Min, *Biomaterials*, 2013, **34**(13), 3503–3510.
36 F. Li, B. Bae and K. Na, *Bioconjugate Chem.*, 2010, **21**(7), 1312–1320.
37 K. W. Lee, D. Jeong and K. Na, *Carbohydr. Polym.*, 2013, **94**, 850–856.
38 J. Lin, K. Wang, H. Wang, Q. Shao, Y. Luan, Y. Xu, X. Song, W. Tan, S. Liu, F. Wei and X. Qu, *Med. Oncol.*, 2017, **34**, 9.
39 M. J. Ryu and H. S. Chung, *Mol. Med. Rep.*, 2016, **14**(4), 3255–3260.